APPLIED ORGANOMETALLIC CHEMISTRY
Appl. Organometal. Chem. 2004; **18**: 244–251
Published online in Wiley InterScience (www.interscience.wiley.com). DOI:10.1002/aoc.616

Structural comparisons between analogously substituted gallane–pnictine adducts

Andreas Kuczkowski, Stephan Schulz* and Martin Nieger

Institut für Anorganische Chemie der Universität Bonn, Gerhard-Domagk-Str. 1, D-53121 Bonn, Germany

Received 11 December 2003; Revised 22 January 2004; Accepted 23 January 2004

The syntheses and solid-state structures of five Lewis acid–base adducts $Et_3Ga–E(SiMe_3)_3$ (E = P (1), As (2), Sb (3)), i-Bu(t-Bu)$_2$Ga–P(i-Pr)$_3$ (4) and (t-Bu)$_3$Ga–As(i-Pr)$_3$ (5) are described and the structural trends observed within these adducts are discussed and compared with those reported for the corresponding alane adducts. Ga–C bond distances and C–Ga–C bond angles were found to be useful structural parameters to estimate the strength of the Lewis acid–base interaction in the solid state. In addition, the solid-state structure of uncomplexed t-Bu$_3$Ga (6) is reported. Copyright © 2004 John Wiley & Sons, Ltd.

KEYWORDS: main group element; Lewis acid; Lewis base; adduct; Group 13; Group 15

INTRODUCTION

Lewis acid–base reactions between Group 13 (R_3M) and Group 15 compounds (R_3E) have been studied for more than two centuries. The first reaction of this type was investigated by Gay-Lussac *et al*.[1] (as cited by Jonas *et al*.[2]) almost 200 years ago, who synthesized the first compound of this type, $F_3B{\cdot}NH_3$. In particular, adducts of the type $R_3M–ER_3$ containing the lighter elements of both groups (M = B, Al; E = N, P) were synthesized and structurally characterized in large numbers (e.g. see the review articles by Jones *et al*.[3] and Gardiner and Raston[4]) and their dissociation enthalpies were determined both experimentally (e.g. see Gur'yanova *et al*.[5]) and by computational studies (e.g. see Refs 6–11 and references cited therein), whereas the corresponding stibine and bismuthine adducts have been investigated to a far lesser extent (e.g. see Refs 12 and 13 and references cited therein). Unfortunately, experimental data on the thermodynamic stability of stibine and bismuthine adducts (dissociation energies) are still virtually unavailable. Since structural parameter obtained from single-crystal X-ray diffraction studies may allow an estimation of the donor–acceptor interaction of such adducts, we became interested in the synthesis of analogously substituted adduct groups. Consequently, we reported on the syntheses and X-ray crystal structures of two alane adducts groups ($Et_3Al–E(SiMe_3)_3$, t-$Bu_3Al–E$(i-Pr)$_3$ (E = P, As, Sb, Bi)).[12] These studies clearly demonstrated that the strength of the donor–acceptor interaction can be estimated following the model described by Haaland.[14] Herein we report on the synthesis and single-crystal X-ray structures of several gallane adducts ($Et_3Ga–E(SiMe_3)_3$, t-$Bu_3Ga–E$(i-Pr)$_3$ (E = P, As, Sb, Bi). (Data sets of t-$Bu_3Ga–P$(i–Pr)$_3$ obtained from single-crystal X-ray diffraction studies showed severe disorder problems and could not be refined. Consequently, we substituted one t-Bu group by an i-Bu group and obtained single crystals of i-Bu(t-Bu)$_2$Ga–P(i-Pr)$_3$, which did not show these problems.) The structural trends found within these adduct groups are compared with the structural parameters as observed for uncomplexed t-Bu_3Ga, whose structure was also determined, and with those obtained for the corresponding alane adducts in order to verify the influence of the central Group 13 element on such interactions.

*Correspondence to: Stephan Schulz, Institut für Chemie der Universität Bonn, Gerhard-Domagk-Str. 1, D-53121 Bonn, Germany.
E-mail: sschulz@uni-bonn.de
Contract/grant sponsor: Deutsche Forschungsgemeinschaft.
Contract/grant sponsor: Fonds der Chemischen Industrie.
Contract/grant sponsor: Bundesministerium für Bildung, Wissenschaft, Forschung und Technologie.

RESULTS AND DISCUSSION

Addition of an equimolar amount of R_3Ga to E(SiMe$_3$)$_3$ (E = P (**1**)), As (**2**)) and to E(i-Pr)$_3$ (E = P (**4**), As (**5**)) resulted in the formation of the corresponding adducts, which were obtained as colorless solids. **1**, **2**, **4** and **5** were recrystallized from solutions in *n*-pentane at −30 °C and characterized

by multinuclear magnetic resonance (^{1}H, ^{13}C (^{31}P)), mass spectroscopy and elemental analysis.

$$R_3Ga + ER'_3 \longrightarrow R_3Ga{-}ER'_3$$
$$E = P, As$$

Compared with the starting compounds, the proton resonances of **1**, **2**, **4** and **5** are slightly shifted downfield (ligands bound to gallium) and upfield (ligands bound to Phosphorous and arsenic), as was observed for the corresponding alane adducts.[12] The ^{31}P NMR resonances of **1** and **4** are shifted to higher field compared with those of $P(SiMe_3)_3$ and $P(i\text{-}Pr)_3$, which is typical for triele–phosphine adducts containing sterically bulky phosphines with increased donor ability.[15] The stability of **1**, **2**, **4** and **5** in the gas phase is rather low, as is indicated by the absence of the molecular ion peaks [M^+] in their mass spectra.

In order to investigate the strength of the acid–base interaction, **1**, **2**, **4** and **5** were studied by single-crystal X-ray diffraction. The corresponding stibine[16,17] and bismuthine adducts[18] have been described previously. The solid-state structure of $Et_3Ga{-}Sb(SiMe_3)_3$ (**3**), which was previously determined by Wells *et al*.[17] at 138 K, was reinvestigated at 123 K. Single crystals of **1**–**5** (Figs 1–5 respectively; Tables 1 and 2) were obtained from solutions in *n*-pentane at −30 °C.

The Ga–P (2.582(1) Å (**1**); 2.720(2) Å (**4**)) and Ga–As bond distances (2.684(1) Å (**2**); 2.905(1) Å (**5**)) are significantly elongated compared with the sum of the covalent radii (Ga–P 2.36 Å; Ga–As 2.47 Å),[19] as is typical for donor–acceptor bonds. Those of **4** and **5**, which contain sterically more demanding organic substituents, are significantly elongated compared with those of **1** and **2** due to increased repulsive steric interactions between the Lewis acid and the Lewis base. To the best of our knowledge, $i\text{-Bu}(t\text{-Bu})_2Ga{-}P(i\text{-Pr})_3$ (**4**) and

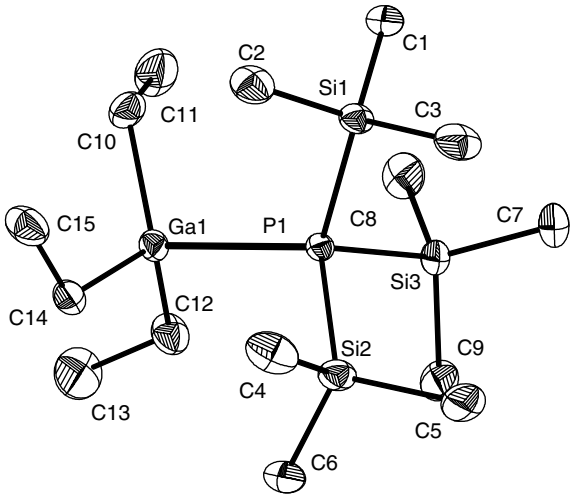

Figure 1. ORTEP plot (50% probability level) showing the solid-state structure and atom numbering scheme for **1**.

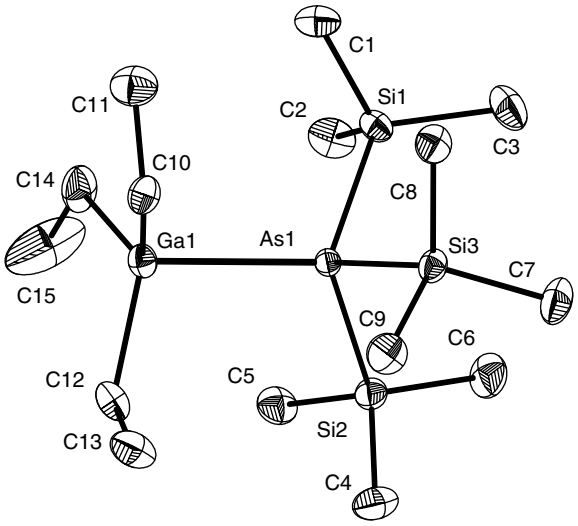

Figure 2. ORTEP plot (50% probability level) showing the solid-state structure and atom numbering scheme for **2**.

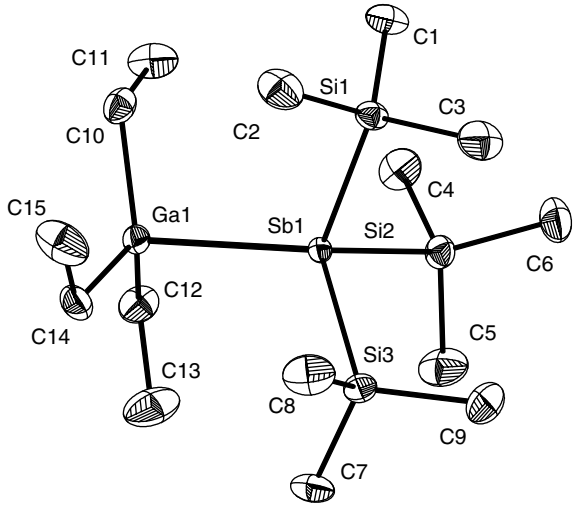

Figure 3. ORTEP plot (50% probability level) showing the solid-state structure and atom numbering scheme for **3**.

$(t\text{-Bu})_3Ga{-}As(i\text{-Pr})_3$ (**5**) show the longest Ga–P and Ga–As bond distances ever observed. The longest Ga–P dative bond reported to date was found for $(Me_3CCH_2)_3Ga{-}PHPh_2$ (2.683(5) Å),[20] whereas Ga–As bond distances observed for gallane–arsine adducts of the types $R_3Ga{-}AsR'_3$ and $I_4Ga_2(AsEt_3)_2$[21] range from 2.423(3) Å ($I_3Ga{-}As(SiMe_3)_3$)[22] to 2.626(1) Å ($(Me_3CCH_2)_3Ga{-}As(SiMe_3)_3$).[23] Despite the increase of the atomic radii from Phosphorous to arsenic, the Ga–As distances are surprisingly shorter than the Ga–P bond lengths observed for phosphane adducts. The longest Ga–As bond distance reported to date was found for the four-membered heterocycle $[t\text{-}Bu_2GaAs(SiMe_3)_2]$ (2.630(1) Å).[24] The Ga–As bond length observed in **5** is about 0.28 Å longer! The Ga–C bond lengths (average values) of $Et_3Ga{-}E(SiMe_3)_3$

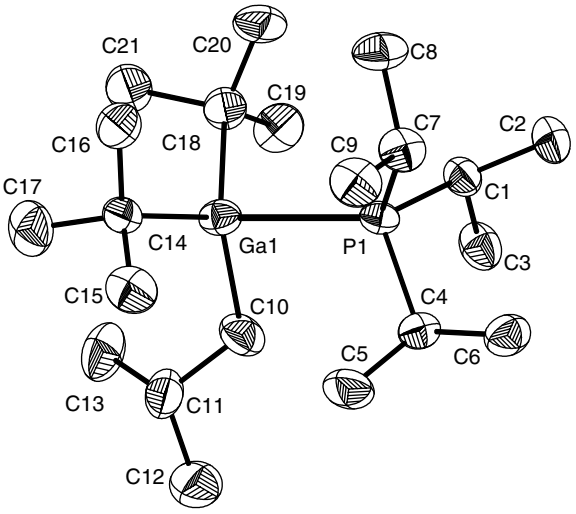

Figure 4. ORTEP plot (50% probability level) showing the solid-state structure and atom numbering scheme for **4**.

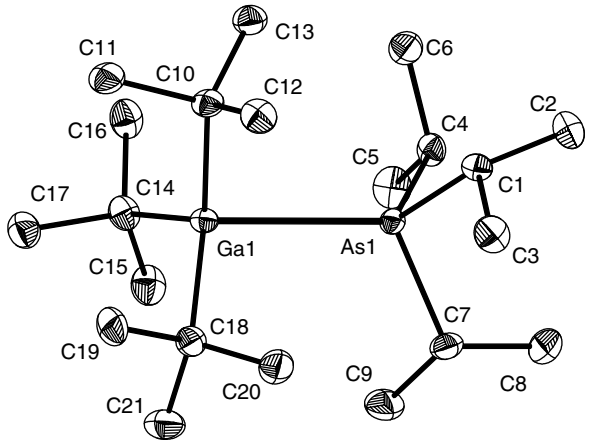

Figure 5. ORTEP plot (50% probability level) showing the solid-state structure and atom numbering scheme for **5**.

adducts (2.004(3) Å (**1**), 2.002(2) Å (**2**), 1.995(5) Å (**3**)) are slightly shorter than those of **4** and **5** (Ga–C 2.044(5) Å (**4**); 2.050(3) Å (**5**)), whereas the sum of the C–Ga–C bond angles observed for **1**–**5** are comparable (343.4° **1**, 345.7° **2**, 349.5° **3**, 346.3° **4**, 344.8° **5**).

Structural trends comparison for $Et_3Ga–E(SiMe_3)_3$ adducts

The Ga–E bond lengths (Fig. 6; Table 3) increase by 0.38 Å (2.582(1) Å **1**; 2.684(1) Å **2**; 2.854(1) Å **3**; 2.966(1) Å (bismuth)). This reflects almost exactly the increase of the sum of the covalent radii from Phosphorous to bismuth (0.4 Å). The average Ga–C bond lengths steadily decrease with increasing atomic number of the pnictine (E = P, 1.989(1) Å

Table 1. Crystallographic data for $Et_3Ga–E(SiMe_3)_3$ (E = P (**1**), As (**2**), Sb (**3**))

	1	**2**	**3**
Molecular formula	$C_{15}H_{42}GaPSi_3$	$C_{15}H_{42}AsGaSi_3$	$C_{15}H_{42}GaSbSi_3$
Formula weight	407.45	451.40	498.23
Crystal system	Monoclinic	Monoclinic	Monoclinic
Space group	$P2(1)/c$ (no. 14)	$P2(1)/c$ (no. 14)	$P2(1)/c$ (no. 14)
a (Å)	14.2672(3)	14.7277(1)	14.9610(1)
b (Å)	9.7671(2)	9.7212(1)	9.9539(1)
c (Å)	16.9756(4)	16.7843(1)	16.9830(1)
β (°)	93.464(2)	91.911(1)	91.748(1)
V (Å^3)	2361.21(9)	2401.69(3)	2527.94(3)
Z	4	4	4
μ (mm^{-1})	1.379	2.656	2.270
D_{calcd} (g cm^{-3})	1.146	1.248	1.309
Crystal dimensions (mm^{-1})	0.35 × 0.12 × 0.08	0.15 × 0.10 × 0.05	0.20 × 0.15 × 0.10
No. of reflections recorded	15 084	50 092	48 474
No. of nonequivalent reflections recorded	4216	4211	4438
R_{merg}	0.0571	0.0503	0.0556
No. of parameters refined/restraints	181/0	181/0	181/0
R_1[a]; wR_2[b]	0.040, 0.102	0.021, 0.052	0.036, 0.100
Goodness of fit[c]	1.13	1.04	1.16
Final max, min $\Delta\rho$ (e − Å^{-3})	0.62, −0.76	0.52, −0.41	2.74 (Sb), −0.98

[a] $R_1 = \sum(||F_o| - |F_c||)/\sum|F_o|$ (for $I > 2\sigma(I)$).
[b] $wR_2 = \{\sum[w(F_o^2 - F_c^2)^2]/\sum[w(F_o^2)^2]\}^{1/2}$.
[c] Goodness of fit $= \{\sum[w(|F_o^2| - |F_c^2|)^2]/(N_{obs} - N_{param})\}^{1/2}$.

Table 2. Crystallographic data for t-Bu_3Ga–E(i-Pr)$_3$ (E = P (**4**), E = As (**5**)) and t-Bu_3Ga (**6**)

	4	**5**	**6**
Molecular formula	$C_{21}H_{48}GaP$	$C_{21}H_{48}AsGa$	$C_{12}H_{27}Ga$
Formula weight	401.28	445.23	241.06
Crystal system	Monoclinic	Monoclinic	Monoclinic
Space group	*Pn* (no. 13)	*P*2(1)/*c* (no. 14)	*Pn* (no. 7)
a (Å)	8.6702(5)	13.5639(2)	15.3118(2)
b (Å)	8.9393(5)	8.8727(1)	8.9405(1)
c (Å)	15.8164(11)	19.8512(3)	31.0767(6)
β (°)	99.588(3)	91.284(1)	99.930(1)
V (Å^3)	1208.73(13)	2388.46(6)	4190.52(11)
Z	2	4	12
μ (mm^{-1})	1.205	2.527	1.934
D_{calcd} (g cm^{-3})	1.103	1.238	1.146
Crystal dimensions (mm^3)	0.20 × 0.10 × 0.05	0.60 × 0.45 × 0.30	0.30 × 0.30 × 0.30
No. of reflections recorded	9117	22 188	31 968
No. of nonequivalent reflections recorded	3784	4200	14 149
R_{merg}	0.0571	0.0921	0.0518
No. of parameters refined/restraints	208/2	208/0	704/2
R_1[a]; wR_2[b]	0.045, 0.078	0.036, 0.094	0.034, 0.068
Goodness of fit[c]	0.93	1.03	0.96
Final max, min $\Delta\rho$ (e − Å^{-3})	0.57, −0.31	0.78, −1.16	0.45, −0.41

[a] $R_1 = \sum(||F_o| - |F_c||)/\sum|F_o|$ (for $I > 2\sigma(I)$).
[b] $wR_2 = \{\sum[w(F_o^2 - F_c^2)^2]/\sum[w(F_o^2)^2]\}^{1/2}$.
[c] Goodness of fit $= \{\sum[w(|F_o^2| - |F_c^2|)^2]/(N_{obs} - N_{param})\}^{1/2}$.

Table 3. Bond distances (Å) and angles (°) of **1**–**5** as determined by single-crystal X-ray diffraction (E = P, As; X = Si, C)

	1	**2**	**3**	**4**	**5**
Ga–E	2.582(1)	2.684(1)	2.854(1)	2.720(1)	2.905(1)
Ga–C	2.002(3)	1.995(2)	1.991(5)	2.032(5)	2.044(3)
Ga–C	2.003(3)	2.005(2)	1.995(5)	2.033(5)	2.048(3)
Ga–C	2.006(3)	2.006(2)	1.999(5)	2.068(5)	2.059(3)
C–Ga–C	118.2(2)	115.4(1)	116.7(2)	116.9(2)	115.2(2)
C–Ga–C	112.7(2)	115.3(1)	116.7(2)	115.4(2)	114.4(2)
C–Ga–C	112.5(2)	115.0(1)	116.1(2)	114.0(3)	115.2(2)
C–Ga–E	117.5(2)	104.2(1)	103.1(2)	108.5(2)	105.3(1)
C–Ga–E	113.1(3)	102.6(1)	100.5(2)	94.1(2)	99.5(1)
C–Ga–E	116.2(2)	101.6(1)	99.3(2)	104.6(2)	104.8(1)
E–X	2.267(2)	2.362(1)	2.553(2)	1.856(4)	1.989(3)
E–X	2.269(2)	2.363(1)	2.561(2)	1.861(5)	1.999(3)
E–X	2.274(2)	2.365(1)	2.563(2)	1.869(5)	2.003(3)
X–E–X	107.4(1)	105.9(1)	103.3(1)	105.2(2)	103.8(2)
X–E–X	105.6(1)	105.0(1)	104.3(1)	103.8(2)	99.8(2)
X–E–X	106.0(1)	104.1(1)	101.8(1)	103.9(2)	102.7(2)
X–E–Ga	115.0(1)	113.5(1)	115.7(1)	113.0(2)	122.2(1)
X–E–Ga	109.9(1)	113.8(1)	115.8(1)	122.9(2)	115.3(1)
X–E–Ga	112.5(1)	113.6(1)	114.3(1)	106.2(2)	110.4(1)

(**1**); Bi, 1.978(1) Å), whereas the sum of the C–Ga–C bond angles increases (E = P, 343.4° (**1**); Bi, 353.9°). Comparable structural trends have been reported for the corresponding alane adducts $Et_3Al–E(SiMe_3)_3$.[12] According to the Haaland model, both the shortening of the Ga–C bond length (Fig. 7) and the widening of the C–Ga–C bond angle (Fig. 8) with increasing atomic number of the pnictine reflect decreasing donor–acceptor interactions.

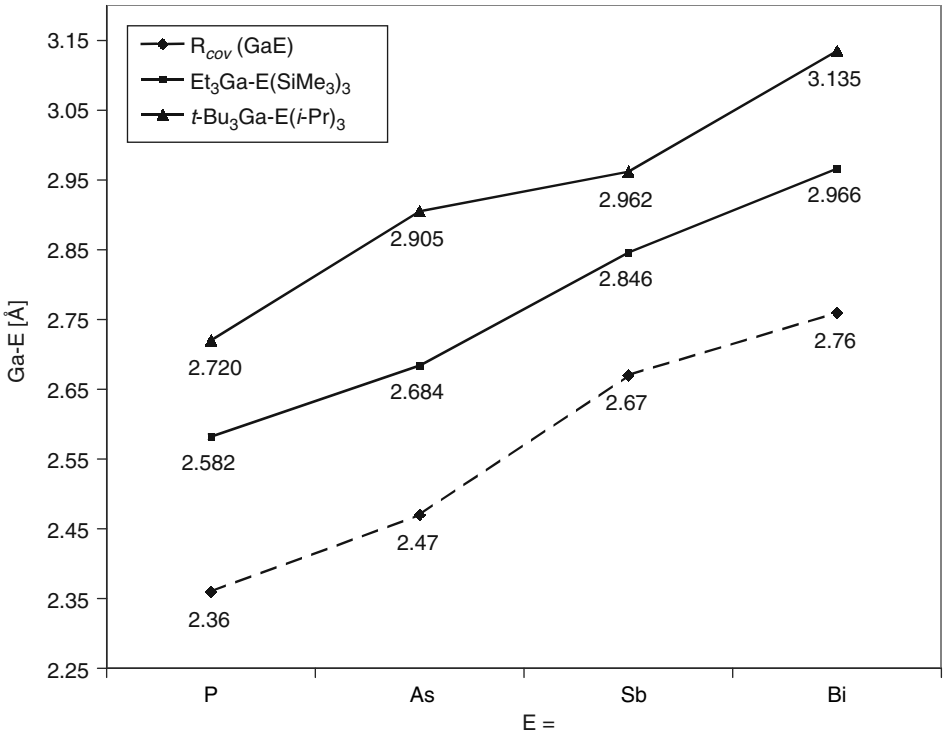

Figure 6. Ga–E bond lengths of $Et_3Ga–E(SiMe_3)_3$ and t-$Bu_3Ga–E$(i-Pr)$_3$ adducts.

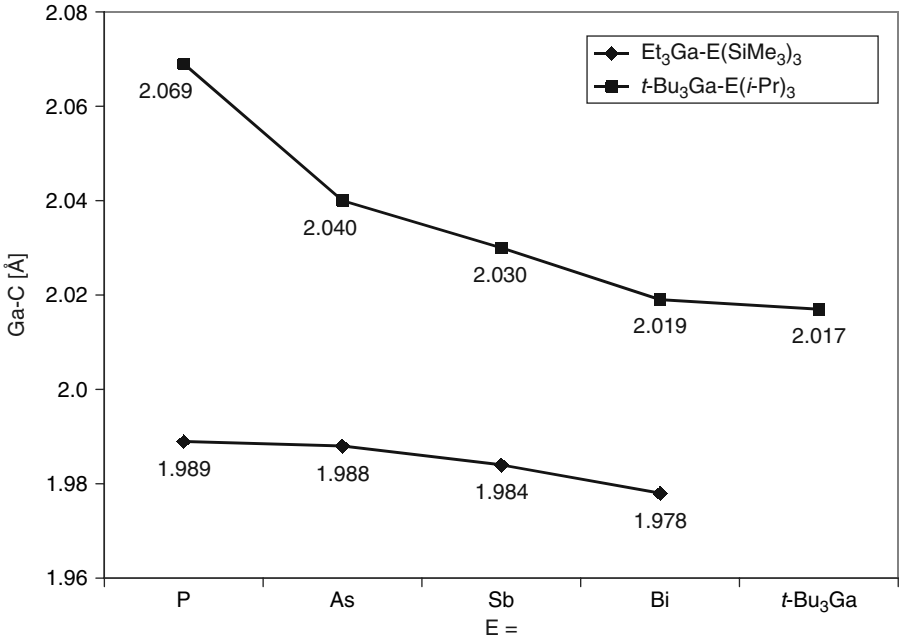

Figure 7. Ga–C bond lengths of $Et_3Ga–E(SiMe_3)_3$ and t-$Bu_3Ga–E$(i-Pr)$_3$ adducts (average values) and t-Bu_3Ga.

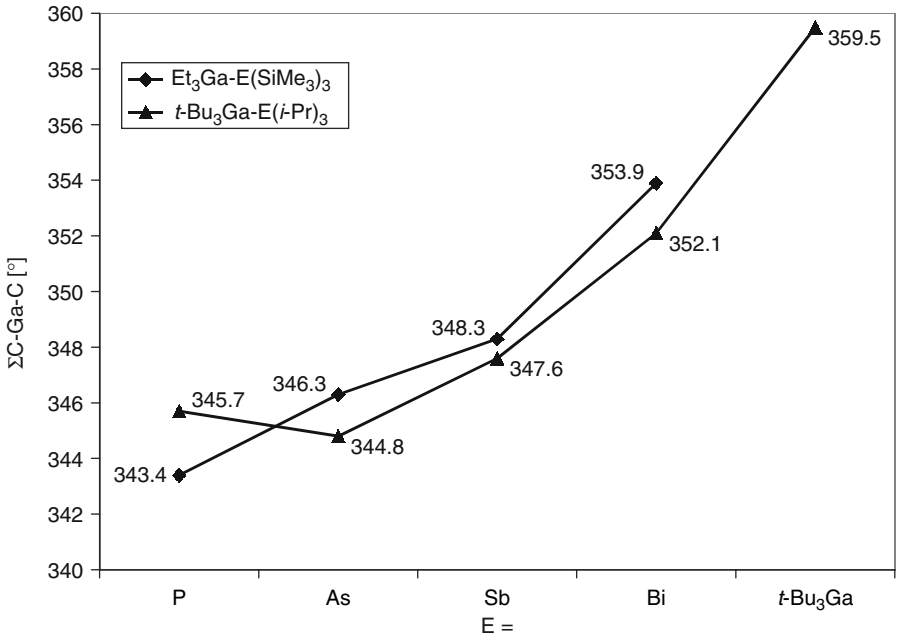

Figure 8. Sum of the C–Ga–C bond angles of $Et_3Ga–E(SiMe_3)_3$ and t-$Bu_3Ga–E(i\text{-}Pr)_3$ adducts and t-Bu_3Ga.

Structural trends comparison for t-Bu_3Ga–$E(i\text{-}Pr)_3$ adducts

As was found for the $Et_3Ga–E(SiMe_3)_3$ adducts, the Ga–C bond lengths decrease and the C–Ga–C bond angles increase with increasing atomic number of the central pnictine. However, owing to the replacement of one t-Bu group by a sterically less demanding i-Bu group in i-Bu(t-Bu)$_2$Ga–P(i-Pr)$_3$ (**4**), the average Ga–C bond length and sum of the C–Ga–C bond angles of **4** do not fit into these trends (see Figs 7 and 8). The Ga–E bond lengths observed for the t-$Bu_3Ga–E(i\text{-}Pr)_3$ adducts are generally longer than those of the $Et_3Ga–E(SiMe_3)_3$ adducts due to increased steric interactions between the bulky organic substituents. In particular, t-$Bu_3Ga–As(i\text{-}Pr)_3$ (**5**; 2.905(1) Å) and t-$Bu_3Ga–Bi(i\text{-}Pr)_3$ (3.135(1) Å) exhibit very long Ga–E bond distances compared with the corresponding $Et_3Ga–E(SiMe_3)_3$ adducts and with the sum of the covalent radii. In addition, the elongation of the Ga–E bond lengths from the phosphine to the bismuthine adduct (0.42 Å) is more pronounced than that observed for the $Et_3Ga–E(SiMe_3)_3$ adducts (Fig. 6). In order to investigate the structural changes due to the adduct formation within the t-$Bu_3Ga–E(i\text{-}Pr)_3$ adducts in more detail, the solid-state structure of t-Bu_3Ga **6** (Fig. 9) was also determined. Single crystals of t-Bu_3Ga (**6**) were grown from a solution in pentane at −40 °C.

t-Bu_3Ga (**6**) crystallizes in the monoclinic space group *Pn* (no. 7) with six independent molecules in the asymmetric unit. The average Ga–C bond length of these molecules ranges from 2.017(4) to 2.022(5) Å and the sum of C–Ga–C bond angles was found to vary from 357.5 to 359.5°. Both the deviation from exact trigonal planar environment (sum of bond angles 360°) and the Ga–C bond length variations result from weak intermolecular interactions between t-Bu_3Ga molecules. Five of the six independent t-Bu_3Ga molecules show weak contacts to adjacent t-Bu_3Ga molecules, with Ga–C bond distances ranging from 3.2 to 3.6 Å, whereas only one t-Bu_3Ga molecule remains uncoordinated. Such weak intermolecular interactions have also been reported for Et_3Ga (Et_3Ga contains four independent molecules in the asymmetric unit, which adopt a layered structure due to the presence of weak Ga–C interactions between each $GaEt_3$ molecule with two $GaEt_3$ neighbors).[25] Compared with the gas-phase structure of t-Bu_3Ga (Ga–C 2.034(2) Å; C–Ga–C 120°; Rankin DWH, personal communication), the average Ga–C bond length observed in the solid state is slightly shorter. The uncoordinated t-Bu_3Ga molecule exhibits the largest sum of the C–Ga–C bond angles (359.5°) and an average Ga–C bond distance of 2.018 Å. The t-$Bu_3Ga–E(i\text{-}Pr)_3$ adducts show longer Ga–C bond lengths and smaller C–Ga–C bond angles. These findings agree very well with the Haaland model and where also observed for the corresponding alane adducts ($Et_3Al–E(SiMe_3)_3$, t-$Bu_3Al–E(i\text{-}Pr)_3$). However, the sum of the C–Ga–C bond angles were found to be generally larger than the sum of the C–Al–C bond angles of the corresponding alane adducts. This is a strong indication for weaker acid–base interactions in gallane adducts compared with alane adducts. These structural findings agree very well with the less-pronounced Lewis acidity of trialkylgallanes compared with trialkylalanes.

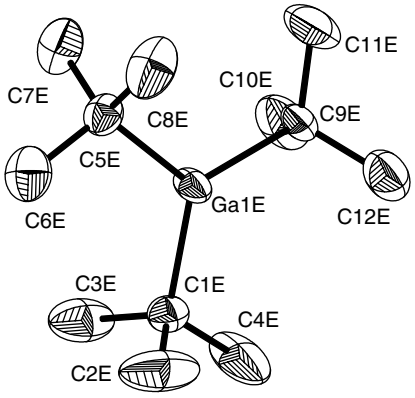

Figure 9. ORTEP plot (50% probability level) showing the solid-state structure and atom numbering scheme for **6**. For clarification, only one of the six independent t-Bu_3Ga molecules is presented. Selected bond lengths (Å) and angles (°): Ga(1E)–C(1E) 2.010(4), Ga(1E)–C(5E) 2.023(4), Ga(1E)–C(9E) 2.022(4); C(1E)–Ga(1E)–C(5E) 120.8(2), C(1E)–Ga(1E)–C(9E) 118.8(2), C(5E)–Ga(1E)–C(9E) 119.9(2).

CONCLUSIONS

The solid-state structures of t-Bu_3Ga and five gallane–pnictine adducts were determined by single-crystal X-ray diffraction. Detailed structural comparisons within analogously substituted adduct groups $Et_3Ga–E(SiMe_3)_3$ and t-$Bu_3Ga–E(i\text{-}Pr)_3$ (E = P, As, Sb, Bi) indicate a steadily decreasing stability of the adduct with increasing atomic number of the central pnictine. Comparisons with analogously substituted alane adducts $Et_3Al–E(SiMe_3)_3$ and t-$Bu_3Al–E(i\text{-}Pr)_3$ revealed the influence of the central Group 13 element on the strength of the donor–acceptor interaction. Based on the structural difference observed in the solid state, gallane adducts were found to be generally weaker than their corresponding alane adducts.

EXPERIMENTAL

General considerations

All manipulations were performed in a glovebox under a nitrogen atmosphere or by standard Schlenk techniques. Et_3Ga,[26] t-Bu_3Ga,[27] $P(SiMe_3)_3$,[28] $As(SiMe_3)_3$,[28] $P(i\text{-}Pr)_3$,[29] and $As(i\text{-}Pr)_3$[30] were prepared by literature methods. ^1H, $^{13}C\{^1H\}$ and $^{31}P\{H\}$ NMR spectra were recorded using a Bruker AMX 300 spectrometer and are referenced to internal C_6D_5H (δ^1H 7.154, $\delta^{13}C$ 128.0) or external H_3PO_4 as appropriate. Melting points were measured in sealed capillaries and are not corrected. Elemental analyses were performed at the Mikroanalytisches Labor der Universität Bonn.

General preparation of $R_3Ga–ER_3$

Pure R_3Ga (2 mmol) and R_3E (2 mmol) were combined in the glovebox. **1**, **2**, **4** and **5** were immediately obtained as white solids, which were dissolved in *n*-pentane (5 ml) and stored at −30 °C. Colorless crystals were formed in almost quantitative yield within 12 h.

$Et_3Ga–P(SiMe_3)_3$ (**1**): $M = 407.45$ g mol^{-1}; m.p. 82–84 °C. Anal. Found: C, 44.01; H, 9.96. $C_{15}H_{42}GaPSi_3$ requires C, 44.20; H, 10.40%. δ_H(300 MHz; solvent C_6D_5H; 25 °C): 0.24 [9H, d, ^3J(HP) 4.8 Hz, Si*Me*$_3$], 0.78 [2H, q, ^3J(HH) 8.0 Hz, *CH*$_2$Me], 1.57 [3H, t, ^3J(HH) 8.0 Hz, CH$_2$*Me*]. $\delta_C\{^1H\}$(80 MHz; solvent C_6D_5H; 25 °C): 3.3 [d, ^2J(CP) 8.8 Hz, Me_3Si/P], 6.7 [s, *C*H$_2$Me$_3$], 12.2 [s, CH$_2$*Me*]. $\delta_P\{H\}$(300 MHz; solvent C_6D_5H; 25 °C): −238.9 [s].

$Et_3Ga–As(SiMe_3)_3$ (**2**): $M = 451.40$ g mol^{-1}; m.p. 133–135 °C. Anal. Found: C, 39.65; H, 9.12. $C_{15}H_{42}AsGaSi_3$ requires C, 39.90; H, 9.40%. δ_H(300 MHz; solvent C_6D_5H; 25 °C): 0.29 [9H, s, Si*Me*$_3$], 0.74 [2H, q, ^3J(HH) 7.9 Hz, *CH*$_2$Me], 1.47 [3H, t, ^3J(HH) 7.9 Hz, CH$_2$*Me*]. $\delta_C\{^1H\}$ (80 MHz; solvent C_6D_5H; 25 °C): 3.9 [s, Si*Me*$_3$], 7.6 [s, *C*H$_2$Me], 12.0 [s, CH$_2$*Me*].

(t-Bu)$_2$i-BuGa–P(i-Pr)$_3$ (**4**): $M = 401.28$ g mol^{-1}; m.p. *ca* −10 °C. Anal. Found: C, 62.31; H, 11.88. $C_{21}H_{48}GaP$ requires C, 62.90; H, 12.10%. δ_H(300 MHz; solvent C_6D_5H; 25 °C): 0.99 [2H, d, ^3J(HH) 6.5 Hz, *CH*$_2$CHMe$_2$], 1.06 [6H, dd, ^3J(HP) 11.7 Hz, ^3J(HH) 7.2 Hz, CH*Me*$_2$], 1.15 [6H, s, CH$_2$CH*Me*$_2$], 1.18 [18H, s, 2 × t-Bu], 1.70 [1H, dsept, ^2J(HP) 2.4 Hz, ^3J(HH) 7.2 Hz, *CH*Me$_2$], 1.98–2.06 [1H, m, CH$_2$*CH*Me$_2$]. $\delta_C\{^1H\}$(80 MHz; solvent C_6D_5H; 25 °C): 20.9 [d, ^2J(CP) 12.9 Hz, CH*Me*$_2$], 22.0 [d, ^1J(CP) 17.5 Hz, CHMe$_2$], 27.9 [s, CH$_2$CHMe$_2$], 28.6 [s, CH$_2$CH*Me*$_2$], 30.9 (s, t-Bu), 32.5 [s, CH$_2$CHMe$_2$]. $\delta_P\{H\}$(300 MHz; solvent C_6D_5H; 25 °C): 19.2 [s].

(t-Bu)$_3$Ga–As(i-Pr)$_3$ (**5**): $M = 445.23$ g mol^{-1}; m.p. *ca* −15 °C. Anal. Found: C, 56.14; H, 10.21. $C_{21}H_{48}AsGa$ requires C, 56.70; H, 10.90%. δ_H(300 MHz; solvent C_6D_5H; 25 °C): 1.14 [6H, d, ^3J(HH) 7.2 Hz, CH*Me*$_2$], 1.17 [9H, s, C*Me*$_3$], 1.73 [1H, sept, ^3J(HH) 7.2 Hz, *CH*Me$_2$]. $\delta_C\{^1H\}$(80 MHz; solvent C_6D_5H; 25 °C): 21.6 [s, CH*Me*$_2$], 22.7 [s, *C*HMe$_2$], 30.9 [s, C*Me*$_3$].

X-ray structure solution and refinement

Crystallographic data of **1**–**3** are summarized in Table 1, and those of **4**–**6** in Table 2. Figures 1–5 and Fig. 9 show the ORTEP diagrams of the solid-state structures of **1**–**6**. Data were collected on a Nonius Kappa-CCD diffractometer at 123(2) K using Mo Kα radiation ($\lambda = 0.710\,73$ Å, $2\theta_{max} = 50.0°$). The structures were solved by direct methods (**3**–**5**) or Patterson methods (**1, 2, 6**) (SHELXS-97)[31] and refined by full-matrix least squares on F^2 (SHELXL-97).[32] Empirical absorption corrections were applied for all compounds except **4**. All non-hydrogen atoms were refined anisotropically and hydrogen atoms by a riding model. The absolute structure of **4** was determined by refinement of the Flack *x*-parameter ($x = 0.044(12)$), whereas that of **6** could not be determined ($x = 0.517(7)$, racemic twin). Crystallographic data of **1**–**6** have been deposited with the Cambridge Crystallographic Data Centre, CCDC nos 215844 (**1**), 215845 (**2**), 215849 (**3**), 215847 (**4**), 215846 (**5**) and 215848 (**6**). Copies of this information may be obtained free of charge from The Director, CCDC, 12 Union Road, Cambridge CB2 1EZ, UK

(Fax: +44-1223-336-033; e-mail: deposit@ccdc.cam.ac.uk; or www: http://www.ccdc. cam.ac.uk).

Acknowledgements

S. S. gratefully acknowledges generous financial support by the Deutsche Forschungsgemeinschaft (DFG), the Fonds der Chemischen Industrie (FCI), the Bundesministerium für Bildung, Wissenschaft, Forschung und Technologie (BMBF) and Professor E. Niecke, Universität Bonn.

REFERENCES

1. Gay-Lussac JL, Thenard JL. *Mem. Phys. Chim. Soc. d'Arcueil* 1809; **2**: 210.
2. Jonas V, Frenking G. *J. Chem. Soc. Chem. Commun.* 1994; 1489.
3. Jones C, Koutsantonis GA, Raston CL. *Polyhedron* 1993; **12**: 1829.
4. Gardiner MG, Raston CL. *Coord. Chem. Rev.* 1997; **166**: 1.
5. Gur'yanova EN, Gol'dshtein IP, Romm IP. *Donor-Acceptor Bond*. John Wiley: New York, 1975.
6. Haaland A. *Angew. Chem. Int. Ed. Engl.* 1989; **28**: 992.
7. Brunel JM, Faure B, Maffei M. *Coord. Chem. Rev.* 1998; **178–180**: 665.
8. Anane H, Jarid A, Boutalib A. *J. Phys. Chem. A* 1999; **103**: 9847.
9. Jarid A, Boutalib A. *J. Phys. Chem. A* 2000; **104**: 9220.
10. Jonas V, Frenking G, Reetz MT. *J. Am. Chem. Soc.* 1994; **116**: 8741.
11. Timoshkin AY, Suvorov AV, Bettinger HF, Schaefer III HF. *J. Am. Chem. Soc.* 1999; **121**: 5687.
12. Kuczkowski A, Schulz S, Nieger M, Schreiner PR. *Organometallics* 2002; **21**: 1408.
13. Schulz S. In *Structure and Bonding*, Vol. 103: *Group 13 Chemistry I: Fundamental New Developments*, Roesky HW, Atwood DA (eds). Springer Verlag: Berlin, 2002; 117–167.
14. Haaland A. In *Coordination Chemistry of Aluminum*, Robinson GH (ed.). VCH: Weinheim, 1993.
15. Barron AR. *J. Chem. Soc. Dalton Trans.* 1988; 3047.
16. Schulz S, Nieger M. *J. Chem. Soc. Dalton Trans.* 2000; 639.
17. Baldwin RA, Foos EE, Wells RL, White PS, Rheingold AL, Yap GPA. *Organometallics* 1996; **15**: 5035.
18. Kuczkowski A, Thomas F, Schulz S, Nieger M. *Organometallics* 2000; **19**: 5758.
19. Hollemann AF, Wiberg E. In *Lehrbuch der Anorganischen Chemie*, 101st edn, Wiberg N (ed.). Walter de Gruyter: Berlin, 1995; 1838.
20. Banks MA, Beachley Jr OT, Maloney JD, Rogers RD. *Polyhedron* 1990; **9**: 335.
21. Beagley B, Godfrey SM, Kelly KJ, Kungwankunakorn S, McAuliffe CA, Pritchard RG. *J. Chem. Soc. Chem. Commun.* 1996; 2179.
22. Johansen JD, McPhail AT, Wells RL. *Adv. Mates. Opt. Electron.* 1992; **1**: 29.
23. Wells RL, McPhail AT, Pasterczyk JW, Alvanipour A. *Organometallics* 1992; **11**: 226.
24. Wells RL, McPhail AT, Alvanipour A. *Polyhedron* 1992; **11**: 839.
25. Mitzel NW, Lustig C, Berger RJF, Runeberg N. *Angew. Chem. Int. Ed. Engl.* 2002; **41**: 2519.
26. Coates GE, Wade K. In *Organometallic Compounds, The Main Group Elements*. Methuen: London, 1967.
27. Schwering H-U, Jungk E, Weidlein J. *J. Organometal. Chem.* 1975; **91**: C4.
28. Hermann WA, Brauer G. In *Synthetic Methods of Organometallic and Inorganic Chemistry (Hermann/Brauer)*, Vol. 3, *Phosphorous, Arsenic, Antimony and Bismuth*. Thieme Verlag: Stuttgart, 1996.
29. *Houben Weyl: Methoden der Organischen Chemie, Band XII/1, Organische Phosphorverbindungen Teil 1*. 4. Auflage. Thieme Verlag: Stuttgart, 1963.
30. *Houben Weyl: Methoden der Organischen Chemie, Metallorganische Verbindungen des Arsens, Antimons und Bismuts*, 4. Auflage. Thieme Verlag: Stuttgart, 1978.
31. Sheldrick GM. *Acta Crystallogr. Sect. A* 1990; **46**: 467.
32. Sheldrick GM. SHELXL-97, program for crystal structure refinement, Universität Göttingen, 1997.

